



# Electrochemical promotion of toluene combustion on an inexpensive metallic catalyst

François Gaillard\*, Ning Li

Institut de recherches sur la catalyse et l'environnement de Lyon (IRCELYON), UMR 5256 CNRS - Université de Lyon, 2 Avenue Albert Einstein, F-69626 Villeurbanne Cedex, France

## ARTICLE INFO

### Article history:

Available online 9 July 2009

### Keywords:

Electrochemical promotion of catalysis

EPOC

Toluene combustion

VOC

Ag

## ABSTRACT

Electrochemical promotion of the complete catalytic oxidation of toluene at 310 °C is reported, using a Ag/YSZ/Ag two electrode system where Ag films were deposited on YSZ from AgNO<sub>3</sub> aqueous solution followed by reduction in H<sub>2</sub>. After on-stream activation, a non-negligible conversion (about 30%) at OCV is reached and then the rate of the catalytic toluene conversion into CO<sub>2</sub> and H<sub>2</sub>O can be multiplied by a factor higher than 1.5, by application of a small negative current (about  $-4 \mu\text{A cm}^{-2}$ ). The associated Faradaic efficiency is very high and may exceed  $-13,000$ .

© 2009 Elsevier B.V. All rights reserved.

## 1. Introduction

From the end of the 20th century, the removal of volatile organic compounds (VOCs) emitted from industrial and domestic processes has drawn a lot of attention. An efficient solution is their catalytic oxidation to H<sub>2</sub>O and CO<sub>2</sub> [1]. Supported Pt and Pd are well-established catalysts for this purpose but the quest for cheaper and more available materials is of ever-increasing importance for tomorrow's applications. Such materials are much less active than Pt or Pd but their performance can be improved by using electrochemical promotion of catalysis (NEMCA or EPOC) [2,3]. During the past years, most of the work on EPOC for hydrocarbon combustion focused on lower molecular weight alkanes or alkenes, such as methane, ethylene, propane, propylene, etc. However, for environment protection purpose, the abatement of aromatic organic compounds is still much more important, because they can be far more harmful. Among these aromatic VOCs, toluene is a very important one because it is mainly released into the atmosphere from industrial (benzene fabrication...) and consumer (evaporation from gasoline...) uses and it can cause central nervous system problems for regular exposure to 100 ppm levels. Studies of EPOC applied to toluene combustion are very scarce. The pioneering one was carried out using RuO<sub>2</sub>/YSZ operated at 400–500 °C [4]. Promotional and non-Faradaic effects were found for both anodic (1.5 V) and cathodic (−1.5 V) polarizations, enhancing the rate of toluene oxidation by factors of 8 and 4, respectively. In a more recent work [5], we explored the

EPOC performance of an Ag/YSZ system and found a significant NEMCA effect when applying negative potential or current at a temperature much lower (300 °C) but still compatible with a sufficient oxygen ions conductivity of YSZ. These results were obtained using an Ag paint as the thin film precursor but such a method also suffers from some drawbacks: (i) the composition of the commercial Ag paste is usually unknown and some organic additives, binders or impurities may lead to catalyst poisoning and (ii) the metallic films prepared by this method need to be pre-treated at high temperatures in air or pure oxygen for the decomposition of the organic compounds. In the specific case of Ag, such a high temperature treatment would lead to a loss of metal by reactive thermal evaporation of the silver oxide (AgO) in a background of molecular oxygen [6]. From a practical point of view, it is necessary to find a simple, efficient and cost-effective way to prepare catalytic films, very similar to the techniques used to obtain DSA<sup>®</sup> coatings [7,8], although such apparently simple techniques may suffer from some difficulties [9]. RuO<sub>2</sub> deposits on YSZ obtained by the thermal decomposition of RuCl<sub>3</sub> precursor [4] or Pt films prepared by impregnation on Na(or K)-β-Al<sub>2</sub>O<sub>3</sub> [10,11] are good examples of the application of such simple and efficient methods in EPOC studies.

## 2. Experimental

### 2.1. Catalyst preparation

The electrochemical catalyst consisted of a thin Ag film (working electrode (WE), geometric area of ca. 2 cm<sup>2</sup>) deposited on one side of a 17 mm diameter and 1 mm thick Y<sub>2</sub>O<sub>3</sub> stabilized ZrO<sub>2</sub> electrolyte disk (YSZ, 8 mol% Y<sub>2</sub>O<sub>3</sub>), with Ag counter

\* Corresponding author. Tel.: +33 4 7244 8066; fax: +33 4 7244 5399.  
E-mail address: [francois.gaillard@ircelyon.univ-lyon1.fr](mailto:francois.gaillard@ircelyon.univ-lyon1.fr) (F. Gaillard).

electrodes (CE) on the other side. No reference electrode was added.

To obtain the Ag film, we adapted a deposition/reduction method similar to the one proposed by Vannice and coworkers [12] to prepare various supported Ag catalysts. As the first step, the Ag film was deposited on the one side of YSZ pellets by direct deposit of 500  $\mu\text{L}$  of a  $\text{AgNO}_3$  (Alfa Aesar # 043087, purity 99.995%) aqueous solution. Such a volume allowed a complete wetting of the pellet surface. A solution at 26.5 g  $\text{AgNO}_3 \text{ L}^{-1}$  was used in order to aim at about 4  $\mu\text{m}$  thick films (thickness is reported to a compact Ag film, considering 10.5 kg  $\text{L}^{-1}$  for Ag density [13]). The disk was then dried in flowing air at 140  $^\circ\text{C}$  for 2 h. Then, 500  $\mu\text{L}$  of the  $\text{AgNO}_3$  aqueous solution was deposited onto the second face of the YSZ pellet, in order to obtain the counter-electrode. The disk was dried again at 140  $^\circ\text{C}$ , then reduced in  $\text{H}_2$  at 300  $^\circ\text{C}$  for 2 h (heating ramp: 2  $^\circ\text{C min}^{-1}$ ) in a quartz reactor and then cooled down to room temperature. After that, the complete system was checked for electrodes electronic conductivity at room temperature and assembly ionic conductivity at 300  $^\circ\text{C}$ . The thickness of the Ag film was estimated as 3.3  $\mu\text{m}$ , from the weight increase of the pellet after impregnation and after reduction, assuming the density of metallic Ag.

## 2.2. Characterization techniques

### 2.2.1. XRD

XRD patterns of the pellet samples were obtained on a Bruker D8 Advance, using the  $\text{Cu K}\alpha$  line (0.15418 nm). The angular scan was performed from 10 $^\circ$  to 70 $^\circ$  (2 $\theta$ ), with 0.02 $^\circ$  steps. The average crystallite size was estimated using the Scherrer equation:

$$D = \frac{0.90\lambda}{\beta \cos \theta}$$

where  $D$  is the average crystallite size (nm),  $\lambda$  the incident wavelength (nm),  $\beta$  the corrected full width at half maximum (radian) and  $\theta$  the Bragg angle.

### 2.2.2. SEM

The Ag/YSZ samples were investigated by SEM using a Jeol JSM-5800LV scanning electron microscope, operated at 20 kV and 75  $\mu\text{A}$  and controlled by SPIRIT (Princeton Gamma Tech) software.

### 2.2.3. TPD, TPO and TPR

For flow TPD experiments, solids were placed on a quartz wool bed in a U-shaped quartz reactor, positioned vertically in a programmable tube furnace. Temperature was measured by two K-type thermocouples contacting the outer part of the reactor. The TPD experiments were performed in He at a flow 30  $\text{mL min}^{-1}$  monitored by a Brooks mass flow controller. A part of the gas exiting the reactor (about 14  $\text{mL min}^{-1}$ ) was sampled by a heated capillary and analyzed by an Inficon Transpector 2 quadrupole mass spectrometer. Signals at  $m/e = 2, 16, 17, 18, 28, 30, 32, 44$  amu, corresponding, respectively to  $\text{H}^+, \text{O}^+, \text{OH}^+, \text{H}_2\text{O}^+, \text{N}_2^+$  or  $\text{CO}^+, \text{NO}^+, \text{O}_2^+$  and  $\text{CO}_2^+$  ions, were recorded. For TPO and TPR experiments, 1%  $\text{O}_2/\text{He}$  and 1%  $\text{H}_2/\text{He}$  mixtures were used, respectively (flow rates: 30  $\text{mL min}^{-1}$ ).

## 2.3. Catalytic tests

The catalytic reaction was carried out using a specific electrochemical glass reactor operating under atmospheric pressure. A schematic drawing of the reactor is shown in Fig. 1. The Ag/YSZ/Ag pellet was deposited on a glass frit with catalyst-working electrode facing downward. A metallic rod allowed: (i) to press the pellet against the frit, (ii) to decrease the dead volume of the reactor and (iii) to establish the electrical contact with the counter-electrode. The rod was made of aluminum, submitted to a previous treatment

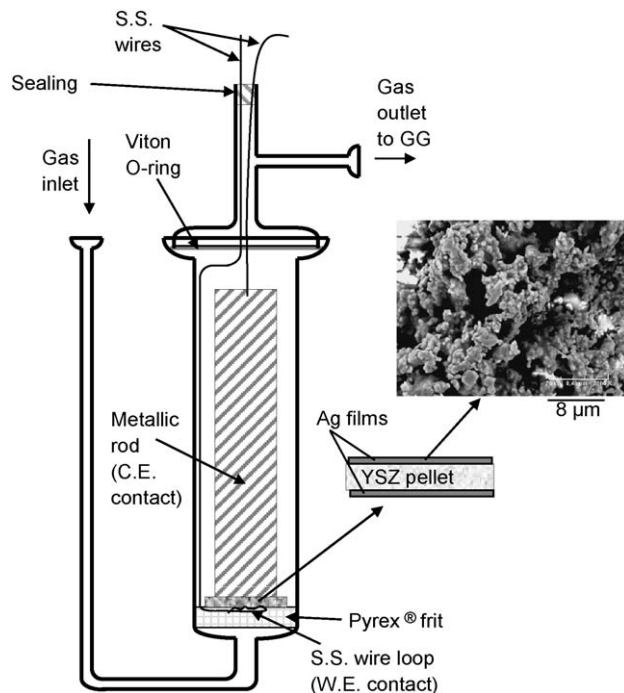


Fig. 1. Schematic drawing of the reactor and sample. SEM micrograph of Ag film.

in air at 300  $^\circ\text{C}$  in order to form a stable alumina layer, not too porous and not too resistive. Electrical contact with the working electrode was made by a loop of stainless steel wire. Therefore, this system is absolutely expensive metal-free provided that neither Au nor Pt was used for the electrodes or for the electrical contacts. A typical SEM micrograph of the Ag film is shown in the inset. As reported in a previous paper [14] the film appeared very porous. XRD and EPMA indicated that it is made of metallic silver. For activity evaluation, a mixture of  $\text{O}_2$ , toluene and He (1%  $\text{O}_2$ , 500 ppm toluene, He as the balance, total flow rate, 100  $\text{mL min}^{-1}$ ) was fed into the reactor. The reactants and products were analyzed by a PerkinElmer Clarus 500 gas chromatograph with a TCD detector. As the major product of the reaction, the yield of  $\text{CO}_2$  was generally used to evaluate the toluene conversion. The CO concentration was always below our detection limit.

A Voltalab<sup>®</sup> system (Radiometer Analytical PGP 201) was used for constant current application and for open voltage measurement.

Two classical parameters were used to describe the magnitude of electrochemical promotion:

- (1) The apparent Faradaic efficiency,  $\Lambda$ , defined from:  $\Lambda = \frac{r-r_0}{I/nF} = \frac{\Delta r}{I/nF}$  where  $r_0$ , in mol O/s (case of an  $\text{O}^{2-}$  conductor), is the catalytic rate at OCV;  $r$  is the catalytic rate under polarization;  $n$  is the number of exchanged electrons during the electrode reaction ( $n = 2$  with an  $\text{O}^{2-}$  conductor) and  $\Delta r$  is the catalytic reaction rate change associated with the current  $I$ . A catalytic reaction exhibits the NEMCA effect when  $|\Lambda| > 1$ . A reaction, which is accelerated by a negative current or overpotential (oxygen removed from the catalyst surface in the present case) with a value of  $\Lambda$  lower than  $-1$  exhibits an electrophilic NEMCA behavior. Conversely, when the catalytic reaction is promoted by a positive current or overpotential (here oxygen supplied to the catalyst surface) with  $\Lambda > 1$ , its NEMCA behavior is called electrophobic.
- (2) The rate enhancement,  $\rho$ , defined from:  $\rho = \frac{r}{r_0}$  where  $r$  is the electro-promoted catalytic rate and  $r_0$  is the unpromoted (open-circuit) catalytic rate.

### 3. Results and discussion

#### 3.1. Ag films elaboration and characterization

As reported in the literature, since the pioneering works of Le Chatelier [15] metallic silver can be obtained by direct decomposition of silver oxide [6,16]. Vannice and coworkers [12] also reported the preparation of supported Ag catalysts by deposition of  $\text{AgNO}_3$  solution followed by drying and reduction. We first investigated the decomposition of bulk  $\text{AgNO}_3$ . A small amount (8.7 mg) of  $\text{AgNO}_3$  was placed onto quartz wool and introduced into a U-shaped quartz tube. Then TPD experiment was carried out under He flow using a heating rate of  $5^\circ\text{C min}^{-1}$ . The TPD profiles are shown in Fig. 2(a) for signals at  $m/e = 18, 30, 32$  and  $44$  amu. Peaks corresponding to simultaneous  $\text{O}_2$  and NO evolution are detected within the temperature range from about 400 to  $500^\circ\text{C}$ . Such profiles and intensity ratio are characteristic of nitrate decomposition [17,18]. Using FTIR spectroscopy, these concomitant desorption peaks were attributed to the decomposition of unidentate or bidentate nitrates [19]. After cooling down to room temperature, TPR run was carried out in 1%  $\text{H}_2$ /He flow using a heating rate of  $20^\circ\text{C min}^{-1}$ . Quantitative approach for  $\text{H}_2$  was made possible by calibrating the MS with pure He and 1 vol.%  $\text{H}_2$ /He using a reactor by-pass and checking for MS linearity in this range. Profiles at  $m/e = 2$  and  $18$  amu during the TPR run are shown in Fig. 2(b). They clearly demonstrate a reduction occurring within a wide range of temperature (from about 200 to  $550^\circ\text{C}$ ). This confirmed by the lower-than-expected amount of  $\text{H}_2$  consumed during the TPR, shows that silver oxide was formed but also that a large part of the initial material was lost by vaporization and condensation on the cold spots of the tubing, as previously reported [6]. Therefore, we investigated the possibility to simultaneously decompose and reduce  $\text{AgNO}_3$  by treating it in a

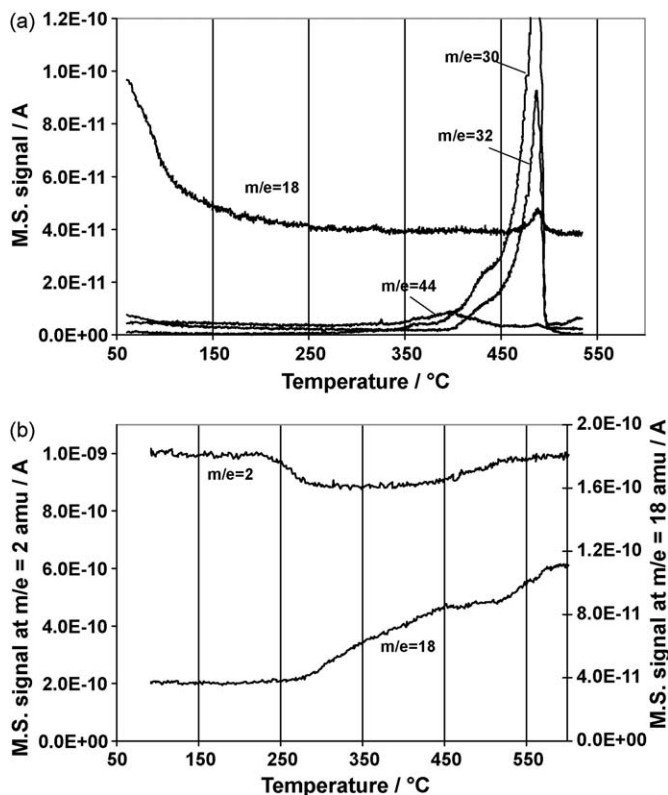


Fig. 2. TPD experiment on  $\text{AgNO}_3$  sample (heating rate:  $5^\circ\text{C min}^{-1}$ , He flow:  $30\text{ mL min}^{-1}$ ) followed by TPR (heating rate:  $20^\circ\text{C min}^{-1}$ , 1%  $\text{H}_2$ -He flow:  $30\text{ mL min}^{-1}$ ).

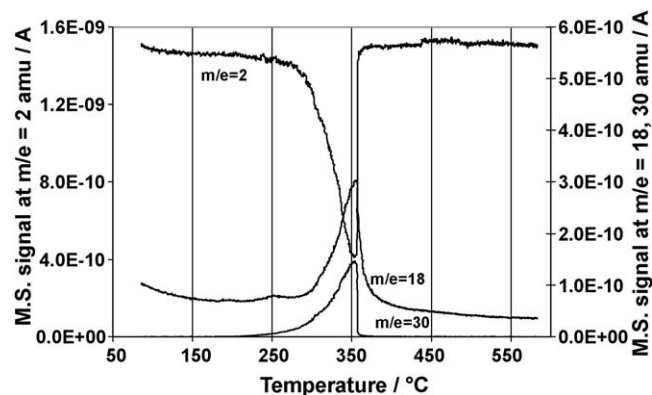


Fig. 3. TPR of  $\text{AgNO}_3$  sample (heating rate:  $5^\circ\text{C min}^{-1}$ , 1%  $\text{H}_2$ -He flow:  $30\text{ mL min}^{-1}$ ).

$\text{H}_2$ -containing flow. The corresponding TPR profiles at  $m/e = 2, 18$  and  $30$  amu are reported in Fig. 3 (8.3 mg sample) and they clearly show a simultaneous decomposition/reduction of  $\text{AgNO}_3$  starting from about  $200^\circ\text{C}$  and briskly stopping at  $370^\circ\text{C}$ . Quantitative approach (after MS standardization using pure He, 1 vol.%  $\text{H}_2$ /He, and 1 vol.%  $\text{O}_2$ /He mixture) and further TPO/TPR runs showed that  $\text{AgNO}_3$  transformation to metallic Ag was complete and that no significant amount of metallic material was lost during the process. In order to simulate what occurs during the processing of a real sample, where  $\text{AgNO}_3$  is deposited on a YSZ pellet from an aqueous solution,  $500\text{ }\mu\text{L}$  of a solution containing  $26.5\text{ g AgNO}_3\text{ L}^{-1}$  were deposited on both the faces of a YSZ pellet, as described above. After drying at  $140^\circ\text{C}$ , the pellet was deposited on a quartz frit in a specially adapted reactor and was submitted to: (i) heating at  $5^\circ\text{C/min}$  under He flow ( $30\text{ mL min}^{-1}$ ) up to  $140^\circ\text{C}$  and (ii) heating at  $5^\circ\text{C/min}$  under 1%  $\text{H}_2$ -He flow ( $30\text{ mL min}^{-1}$ ) up to  $300^\circ\text{C}$  with a 30 min plateau at this temperature. These conditions were a bit different from those employed during the real process (heating rate:  $2^\circ\text{C/min}$  and pure  $\text{H}_2$ ) because we needed to cope with the requirements of continuous MS analysis. Plots of temperature and signals at  $m/e = 2, 18$  and  $30$  amu with respect to treatment time are shown in Fig. 4. One can note that temperature profile is not really satisfying, due to regulation parameters not very adapted to isothermal maintains at quite low temperatures. Nevertheless, it clearly appears that total decomposition/reduction of  $\text{AgNO}_3$  to metallic Ag is performed under these conditions for temperatures not exceeding  $300^\circ\text{C}$ . After removal of the sample, the deposited film exhibited a very good electrical conductivity.

The quantification of superficial metallic Ag ( $\text{Ag}^0$ ) sites is of great important to assess the performance of the catalyst. For this purpose, Vannice and coworkers [20,21] suggested to use  $\text{O}_2$

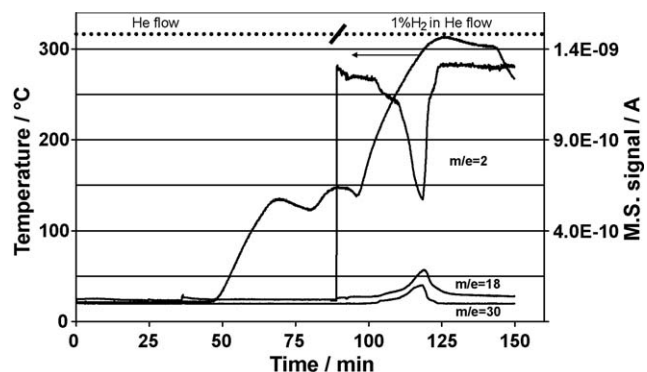


Fig. 4. Processing of  $\text{AgNO}_3$  deposited (from aqueous solution) onto YSZ pellet followed by M.S.

chemisorption at 170 °C followed by titration by H<sub>2</sub> of the adsorbed oxygen species. As underlined by Bianchi and coworkers [22], the adsorption temperature  $T_a = 170$  °C seems to be the best compromise between the fact that O<sub>2</sub> adsorption on Ag is an activated process and that bulk Ag<sub>2</sub>O is likely to be formed at higher  $T_a$ . According to the Vannice group, the stoichiometry of O<sub>2</sub> adsorption is:



and titration of the O<sub>ads</sub> species performs according to:



Repetitive cycles of successive O<sub>2</sub> adsorption and titration by H<sub>2</sub> were performed and analysis carried out by MS, according to a procedure previously described [23]. As the number of Ag<sup>0</sup> sites is expected to be very low, we had to use a reactor with a very small dead volume (about 0.2 mL) to increase sensitivity. Then the silver films had to be scratched from the YSZ pellet (including a part of the support) and put in this reactor between two pieces of quartz wool. For the same reason, the experiment was repeated six times. A typical adsorption/reduction cycle is shown in Fig. 5. First, the O<sub>2</sub>/He mixture flow (30.1 mL min<sup>-1</sup> corresponding to 0.2052 μmol O<sub>2</sub> s<sup>-1</sup>) was established, by-passing the reactor, and was analyzed by the mass spectrometer in order to provide reference signal level for quantitative oxygen analysis. During this time, the reactor was flushed with pure He. Then, the mixture was passed through the reactor (shown by a “A” mark in Fig. 5) and the amount of oxygen both adsorbed (irreversibly and reversibly) and necessary to fill the reactor volume was determined by integration of peak O<sub>1</sub>. Then the reactor was by-passed again (shown by a “B” mark in Fig. 5) and purged by He during a time sufficient to remove all O<sub>2</sub> not irreversibly adsorbed. The mixture was passed again through the reactor (shown by a second “A” mark in Fig. 5) and the amount of oxygen both reversibly adsorbed and necessary to fill the reactor volume was determined by integration of peak O<sub>2</sub>. The peak area difference  $\text{AO}_1 - \text{AO}_2$  directly gives the O<sub>2</sub> amount irreversibly adsorbed at 170 °C and consequently the value of Ag<sup>0</sup> using Eq. (1). In a similar way, using a H<sub>2</sub>/He mixture (27.3 mL min<sup>-1</sup> corresponding to 0.1859 μmol H<sub>2</sub> s<sup>-1</sup>), the peak area difference  $\text{AH}_1 - \text{AH}_2$  gives the H<sub>2</sub> amount necessary to titrate the adsorbed oxygen species, according to Eq. (2). In the present case, we can only obtain by this method a rough determination of the number of Ag<sup>0</sup> sites, because of the detection limits of the MS and possible material loss when recovering the Ag films and transferring them to the reactor. Nevertheless, average values  $\text{AO}_1 - \text{AO}_2 = 1.5 \pm 0.5$  μmol O<sub>2</sub> and  $\text{AH}_1 - \text{AH}_2 = 2.6 \pm 0.3$  μmol H<sub>2</sub>

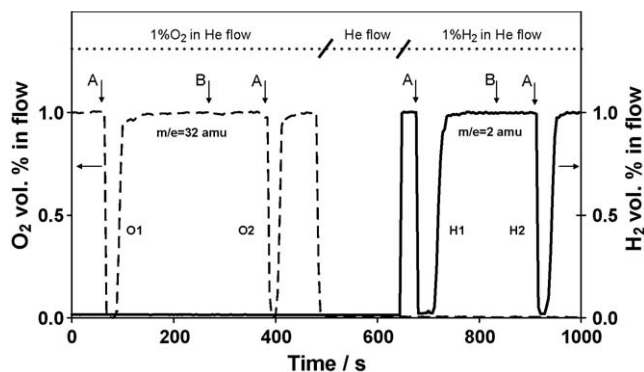


**Fig. 5.** O<sub>2</sub> chemisorption on Ag<sup>0</sup> sites followed by H<sub>2</sub> titration of adsorbed oxygen species (Ag films deposited on YSZ were scratched for this purpose). A: gas mixture sent toward reactor and B: gas mixture sent toward by-pass and reactor purged under pure helium flow.

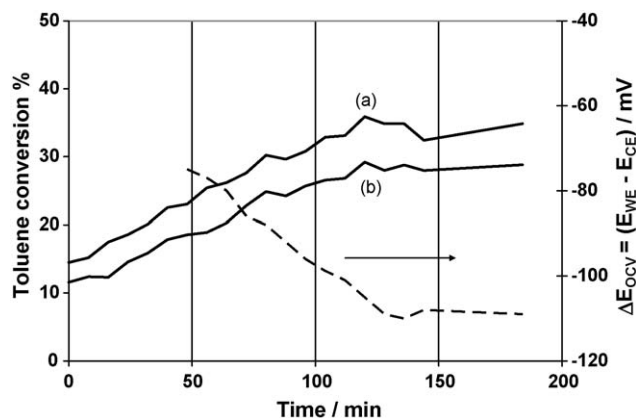


**Fig. 6.** Toluene conversion (calculated from (a) CO<sub>2</sub> production and (b) toluene consumption) and potential difference change during the early stage of the catalytic test at 310 °C (1% O<sub>2</sub>, 500 ppm toluene, He as the balance, total flow rate, 100 mL min<sup>-1</sup>).

were obtained. If we consider 2.6 μmol H<sub>2</sub> as the most accurate value, as it is justified by the stoichiometries considered above, and if we admit that we recovered twice  $7.8 \times 10^{-5}$  mol Ag from the surface films (determined from the volume of AgNO<sub>3</sub> solution initially deposited on each face and confirmed by mass increase), this leads to a dispersion value of about 1.5–2%. This value corresponds to particles about 70 nm in diameter, very compatible with results obtained from XRD [14] and with some results of Vannice and coworkers on Ag/SiO<sub>2</sub> systems [20] using specific reduction conditions.

### 3.2. Catalytic performances

As a preliminary work, we investigated the activity of the empty reactor for toluene combustion. Conversely to what we observed in previous studies [14,5] using a different reactor [24] a noticeable toluene conversion was detected from 290 °C and reached about 8% at 310 °C. Blank experiments were performed with and without the aluminum rod to check that no additional toluene conversion could be attributable to the metal itself. Then the reactor was loaded with a Ag/YSZ/Ag pellet. The thickness of the catalyst-electrode film was 3.3 μm as determined by weighting (for 4.0 μm expected) and thickness of the counter-electrode film was 3.6 μm (for 4.0 μm expected). The sample was heated at 5 °C min<sup>-1</sup> up to 310 °C in He flow (100 mL min<sup>-1</sup>) and then the reactive mixture was admitted to the reactor. In Fig. 6 is plotted toluene conversion, calculated from both CO<sub>2</sub> production (a) and toluene consumption (b). We observe a discrepancy according to the calculation method used. If some parallel reaction was taking place, or if toluene condensation occurred between the reactor and the gas chromatograph, the conversion calculated from toluene consumption would be higher than those calculated using the CO<sub>2</sub> production. Moreover, it is worth noting that both traces vary in very parallel ways and that the values obtained from toluene consumption just appear as shifted by –5% conversion or so. This also rules out any significant parallel reaction and toluene adsorption or desorption from walls and tubing during the catalytic test. The explanation for this observation is that the signal considered as a reference for 500 ppm toluene was obtained at the very beginning of the experiment, by-passing the reactor, with tubing and walls not saturated. Therefore, the actual concentration taken as reference was lower-than-expected (maybe 400 ppm or so) and subsequent values obtained during the catalytic test overestimate the toluene concentration and then underestimate the conversion values.

Such an observation highlights the difficulty to carry out toluene calibration at such low concentrations and it is the reason why, for the following of this paper, conversion and reaction rate



are calculated from the  $\text{CO}_2$  signal, which gives more accurate values. After admitting the reactive mixture to the reactor and waiting for stream stabilization, the conversion is measured ( $t = 0$ ). The corresponding toluene conversion value (about 15%) is slightly above the one recorded with empty reactor, showing a moderate activity of the silver film. Along the time, the conversion value regularly increases to reach about 30% after 2 h on stream and then stabilizes. Such a behavior was reported by many authors on silver catalysts, for example concerning CO oxidation [22],  $\text{CH}_4$  deep oxidation [25] or hydrogen dissociation [26] and was attributed to structure and grain size changes of the silver surface. Although we did not use a conventional three-electrode electrochemical system and no real reference electrode, it is interesting to consider the potential difference ( $\Delta E_{\text{OCV}}$ ) between the catalyst-electrode (WE, pressed against the frit) and the counter-electrode (CE, pressed against the metallic rod). As the two electrodes are of the same material and of similar thicknesses,  $\Delta E_{\text{OCV}}$  is expected to be constant and near-zero. Nevertheless,  $\Delta E_{\text{OCV}}$  value was quite unstable around  $-50$  mV at the beginning of the experiment and after that continuously decreases when toluene conversion increases and then stabilizes at about  $-110$  mV when toluene conversion stabilizes. This behavior is very consistent with what we observed with a Ag/YSZ/Au system [14] and indicates that the two electrodes are not equivalent with respect to the catalytic reaction and that WE activates on stream and is likely to be responsible for the main part of the catalytic process. This is fully justified by the cell geometry and stream accessibility to each electrode. As the counter-electrode is pressed against the metallic rod and faces a very confined volume, it is likely that almost the totality of toluene conversion is insured by the working electrode, which faces the incoming gas stream. Therefore free potential change and stabilization may be considered as a good qualitative indicator of WE on-stream activation and conversion stabilization. As shown later in the text, the absence of promotional effect when positive currents are used also indicates that the counter-electrode participation to overall toluene conversion is not significant.

As shown in Fig. 7, applying a negative small current ( $-2 \mu\text{A}$ ) to the catalyst-electrode significantly increases the toluene conversion. Over it, toluene conversion increases from about 34% to reach about 55% after 25 min and then remains quite stable. The corresponding value  $\rho = 1.6$  could seem quite low, but it is noteworthy to recall that initial OCV conversion was quite high. After the stabilization of activity, the calculated Faradaic efficiency  $\Lambda$  was about  $-13,000$ , which means that the promotion is strongly non-Faradaic. It is worthy mentioning that such a Faradaic efficiency is similar to the values we reported for paste-made Ag film catalyst ( $\Lambda$  ranging from  $-2100$  to  $-39,700$ ) [5]. The toluene conversion

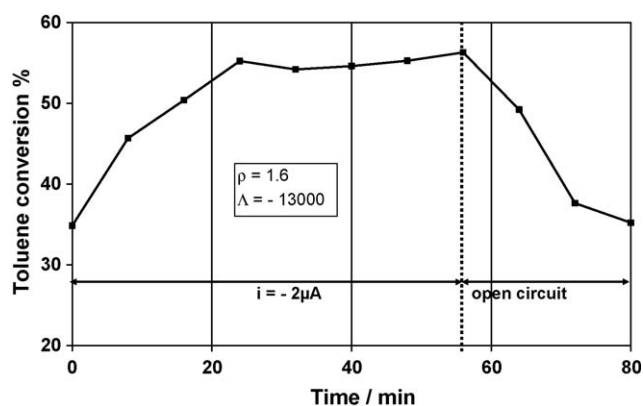


Fig. 7. Effect of  $-2 \mu\text{A}$  on the activity of Ag film catalyst deposited on YSZ pellet. Reaction condition: 1%  $\text{O}_2$ , 500 ppm toluene, He balance; total flow rate,  $100 \text{ mL min}^{-1}$ ,  $310^\circ\text{C}$ .

value is shown to recover quite quickly its initial value upon turning the electrical current off. This experiment can be totally repeated and similar results were obtained when the current is turned on again, indicating it is a repeatable, reversible and non-permanent effect. Applying positive currents ( $+2$ ,  $+10$  and  $+20 \mu\text{A}$ ) to the catalyst-electrode does not increase nor decrease significantly the value of toluene conversion. This proves that the enhancement occurs when oxygen ions species are drawn from the catalyst surface, as reported previously with non-symmetrical Ag/YSZ/Au systems with Ag films obtained either by a paste [5] or by decomposition/reduction of  $\text{AgNO}_3$  [14]. As electro-promotion appears only for negative currents, one could expect a promotional effect from the counter-electrode when positive current is applied. As no promotional effect is observed in this case, it proves that CE faces a very confined volume and that the participation of the counter-electrode is negligible as also suggested by results reported in Fig. 6. According to the rules of EPOC established by Vayenas and coworkers [27], the promotion of toluene catalytic combustion over Ag film catalyst follows an electrophilic NEMCA behavior which can be observed when the electron-donor reactant is more strongly adsorbed on the catalyst surface than the electron-acceptor reactant. These results can be explained by the fact that toluene is a non-saturated hydrocarbon and has  $\pi$ -electrons in its structure, which make it strongly adsorbed on the surface of Ag as an electron-donor therefore hindering the adsorption of  $\text{O}_2$  (an electron-acceptor). The application of a negative potential or current leads to the migration (by electrochemical pumping) of  $\text{O}^{2-}$  from the surface of Ag catalyst, thus changes the work function and favours the adsorption of oxygen.

The results reported in Fig. 8 show the effect of various values of the negative current applied to the catalyst-electrode:  $-2$ ,  $-4$ ,  $-10$ ,  $-20$  and  $-40 \mu\text{A}$ . With respect to toluene conversion, the three intermediate experiments ( $-4$ ,  $-10$ , and  $-20 \mu\text{A}$ ) do not exhibit much difference. Conversely to what is often observed, the value of imposed current does not influence much the time necessary to reach the maximal conversion. This can be attributable to the very porous nature of the film and the necessary time to reach a steady state once the current is established. This chemical phenomenon is more likely to be rate determinant than the electrical one. We did not report on the figures the values of  $\Delta E_{\text{WE-CE}}$ , the potential difference between WE and CE, because it is mainly governed by the ohmic drop within the YSZ pellet, the resistance of which is very high for such low temperatures. Typically,  $\Delta E_{\text{WE-CE}}$  reached its maximal value in less than 1 min after applying the current. Recorded  $\Delta E_{\text{WE-CE}}$  values were repeatable for each current (within  $\pm 5\%$ ):  $-680$  mV for  $-4 \mu\text{A}$ ,  $-890$  mV for  $-10 \mu\text{A}$ ,  $-1800$  mV for  $-20 \mu\text{A}$ , and  $-2400$  mV for  $-40 \mu\text{A}$ . After turning off the current,  $\Delta E_{\text{WE-CE}}$  values

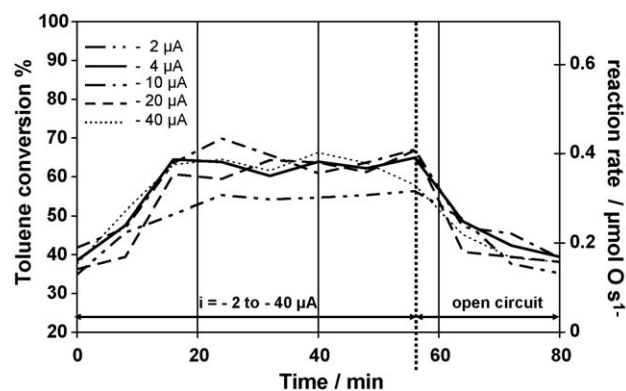


Fig. 8. Effect of various negative currents on the activity of Ag film catalyst deposited on YSZ pellet. Reaction condition: 1%  $\text{O}_2$ , 500 ppm toluene, He balance; total flow rate,  $100 \text{ mL min}^{-1}$ ,  $310^\circ\text{C}$ .

**Table 1**

Maximal toluene conversion, rate enhancement ( $\rho$ ) and Faradaic efficiency ( $\Delta$ ) values from results of Fig. 8.

Current ( $\mu\text{A}$ )	Max. toluene conversion (%)	$\rho$	$\Delta$
–2	55	1.6	–13,000
–4	64	1.7	–8,200
–10	66	1.6	–3,100
–20	64	1.8	–1,800
–40	65	1.7	–900

sharply decreased in some seconds and then free potential recovered its initial value after 15–20 min, according to a curve similar to conversion vs time. Obviously, using  $-2 \mu\text{A}$  is not enough under those initial activity and high ghsv ( $7.5 \times 10^6 \text{ h}^{-1}$  referred to the volume of the active phase) conditions to reach an optimal promotion. For the highest current value ( $-40 \mu\text{A}$ ) toluene conversion starts decreasing before current is turned off. This current value seems too high, but no explanation can be given for this phenomenon since no reversible damage to the system was observed. Corresponding rate enhancement ( $\rho$ ) and Faradaic efficiency ( $\Delta$ ) values are gathered in Table 1. Obviously, maximal toluene conversion is limited by a non-catalytic phenomenon, probably the fact that catalyst surface is only “licked” by the reactant stream and that a non-negligible part of it can by-pass the catalyst. Therefore, the apparent value of  $\Delta$  is the highest for the lowest currents. Nevertheless, the use of a  $-4 \mu\text{A}$  current seems to be a good practical choice under such experimental conditions allowing long time operation (4 h tests were ran) with neither toluene conversion decrease nor permanent promotional effect when current is turned off.

#### 4. Conclusion

A significant NEMCA effect was achieved over a silver catalyst-electrode deposited onto YSZ from a  $\text{AgNO}_3$  aqueous solution followed by  $\text{H}_2$  reduction. After applying negative potential, prominent rate enhancement and high Faradaic efficiency up to –13,000 can be reached. This Faradaic efficiency value is comparable to what we reported for  $\text{Ag/YSZ/Au}$  systems where  $\text{Ad}$  was deposited either from a paste [5] or by a deposition/reduction technique [14]. Taking into account the simple manipulation and cost-efficiency of the deposition/reduction technique, and the ability to work with a system which does not contain any expensive metal, we think it is a method to be considered to elaborate EPOC systems used for the environmentally important application of the total oxidation of aromatic VOC's as toluene.

#### Acknowledgements

The European Commission is acknowledged for Marie Curie Incoming International Fellowships (IIF) to support Dr. Ning Li's research work in France. This work was partially funded by the French “Ministère Délégué à la Recherche” in the framework of the “Action Concertée Incitative Energie, Conception Durable”, grant no. ECD 048. Pr D. Bianchi (IRCELYON) is warmly acknowledged for valuable advices on silver catalysts characterization. The authors are also pleased to thank Dr Antoinette Boréave (IRCELYON) for technical assistance and fruitful discussion, Mrs Laurence Burel (IRCELYON) for performing SEM characterization and Mr M. Hénault and Dr C. Steil (LEPMI, CNRS-INPG, Grenoble, France) for YSZ pellets elaboration.

#### References

- [1] J.J. Spivey, *Ind. Eng. Chem. Res.* 26 (1987) 2165.
- [2] M. Stoukides, C.G. Vayenas, *J. Catal.* 70 (1981) 137.
- [3] C.G. Vayenas, S. Bebelis, S. Ladas, *Nature* 343 (1990) 625.
- [4] I. Constantinou, I. Bolzonella, C. Pliangos, Ch. Comninellis, C.G. Vayenas, *Catal. Lett.* 100 (2005) 125.
- [5] N. Li, F. Gaillard, A. Boréave, *Catal. Commun.* 9 (2008) 1439.
- [6] M.F. Al-Kuhaili, *J. Phys. D: Appl. Phys.* 40 (2007) 2847.
- [7] W.T. Grubb, *Nature* 198 (1963) 883.
- [8] S. Trasatti, *Electrochim. Acta* 45 (2000) 2377.
- [9] C. Comninellis, G.P. Vercesi, *J. Appl. Electrochem.* 21 (1991) 136.
- [10] F. Dorado, A. de Lucas-Consuegra, C. Jiménez, J.L. Valverde, *Appl. Catal. A: Gen.* 321 (2007) 86.
- [11] A. de Lucas-Consuegra, F. Dorado, C. Jiménez-Borja, J.L. Valverde, *Appl. Catal. B: Environ.* 78 (2007) 222.
- [12] L.M. Strubinger, G.L. Geoffroy, M.A. Vannice, *J. Catal.* 96 (1985) 72.
- [13] R.C. Weast, *Handbook of Chemistry and Physics*, 59th ed. CRC Press, West Palm Beach, B-162, 1978.
- [14] N. Li, F. Gaillard, *Appl. Catal. B: Environ.* 88 (2009) 152.
- [15] H. Le Chatelier, *Z. Phys. Chem.* 1 (1887) 516.
- [16] B.V. L'vov, *Thermochim. Acta* 333 (1999) 13.
- [17] S.J. Huang, A.B. Walters, M.A. Vannice, *J. Catal.* 192 (2000) 29.
- [18] S. Benard, L. Retaillieu, F. Gaillard, P. Vernoux, A. Giroir-Fendler, *Appl. Catal. B: Environ.* 55 (2005) 11.
- [19] M. Simokawabe, M. Hatakeyama, K. Shimada, K. Tadokoro, N. Takezawa, *Appl. Catal. A: Gen.* 87 (1992) 205.
- [20] S.R. Seyedmonir, D.E. Strohmayer, G.L. Geoffroy, M.A. Vannice, H.W. Young, J.W. Linowski, *J. Catal.* 87 (1984) 424.
- [21] L.M. Strubinger, G.L. Geoffroy, M.A. Vannice, *J. Catal.* 95 (1985) 72.
- [22] P. Gravejat, S. Derrouiche, D. Farrusseng, K. Lombaert, C. Mirodatos, D. Bianchi, *J. Phys. Chem. C* 111 (2007) 9496.
- [23] M. Rassoul, F. Gaillard, E. Garbowski, M. Primet, *J. Catal.* 203 (2001) 232.
- [24] P. Vernoux, F. Gaillard, L. Bultel, E. Siebert, M. Primet, *J. Catal.* 208 (2002) 412.
- [25] Lj. Kundakov, M. Flytzani-Stephanopoulos, *Appl. Catal. A: Gen.* 183 (1999) 35.
- [26] A.B. Mohammad, I.V. Yudanov, K.H. Lim, K.M. Neyman, N. Rosch, *J. Phys. Chem. C* 112 (2008) 1628.
- [27] C.G. Vayenas, S. Brosda, C. Pliangos, *J. Catal.* 203 (2001) 329.